Spectroscopic Analysis of Chrysotile Asbestos and its Environmental Resistance in Asbestos Cement Waste Products

Gergely Zoltán Macher[1]*, Fanni Károly[2], Christopher Teh Boon Sung[3,4], Dóra Beke[4], András Torma[1] and Szilveszter Gergely[5]

[1]*Department of Applied Sustainability, Széchenyi István University, Hungary*
[2]*Faculty of Engineering, University of Pannonia, Hungary*
[3]*Department of Land Management, Faculty of Agriculture, Universiti Putra Malaysia, 43400 UPM, Serdang, Selangor, Malaysia*
[4]*Department of Plant Sciences, Széchenyi István University, Hungary*
[5]*Department of Applied Biotechnology and Food Science, Budapest University of Technology and Economics, Hungary*

ABSTRACT

Most asbestos-related studies have focused on asbestos exposure risks, their associated health implications, and waste management issues. Our research introduced a unique perspective that has rarely been explored: the impact of environmental factors on asbestos cement products. The novelty of the study is that, in contrast to previous research, in addition to determining the material quality of asbestos, it analyses the trace materials, additives and the emissive nature of chrysotile fibers. This study aims to identify the chrysotile-asbestos content in three common asbestos cement products found in Hungary, with regard to the release of their fibers upon exposure to the environment and to identify trace elements that could be used to identify the origin and function of each of these products. Our analyses revealed the presence of chrysotile in each tested sample, with spectral matches ranging from 59.6% to 86.7%. Asbestos cement products exposed to various environmental influences for long periods showed a greater chrysotile emission capacity than those unexposed or hermetically sealed ones. Additionally, we established that all asbestos cement products contained glass fibers, with an average spectral match of 62.1%. We further identified polysilicate in the materials with an average spectral match of 66.0%, as it was included in asbestos cement

Gergely Zoltán Macher, Fanni Károly, Christopher Teh Boon Sung, Dóra Beke, András Torma and Szilveszter Gergely

products to enhance their heat resistance. Our results pave the way for a new methodology for assessing asbestos cement products with regard to the implementation of their trace element level assessments.

Keywords: Asbestos, chrysotile asbestos, environmental resistance, FTIR, glass fiber, polysilicate

INTRODUCTION

Asbestos is a commercial term for a set of naturally occurring minerals with unique chemical and physical properties (Kusiorowski et al., 2023; Misseri, 2023). These minerals, including chrysotile, amosite, crocidolite, actinolite, tremolite, and anthophyllite, have fibrous appearances and are known as silicate minerals (Tóth & Weiszburg, 2011). They can be classified into two categories: serpentines (sheet silicates) and amphiboles (chain silicates) (Ristić et al., 2011). The term 'asbestiform' is often used to describe their fibrous morphology (Zholobenko et al., 2021). These minerals are characterized by their ability to be separated into long, silky fibers resistant to traction and heat and almost chemically inert (Malinconico et al., 2022).

Asbestos use can be traced back to ancient times (Lavento & Hornytzkyj, 1995; Virta, 2005), but the understanding of the elemental compositions and crystal structures of amphibole and serpentine minerals has only spanned since the 19th century (Ross et al., 2008). Asbestos comprises hydrated silicates of magnesium, iron, calcium, and sodium. The chemical composition of amphibole asbestos (except chrysotile) is $M_7Si_8O_{22}(OH)_2$, with the "M" representing metal cations such as calcium, iron, magnesium, or sodium. Chrysotile, a serpentine mineral, has a distinctive $Mg_3Si_2O_5(OH)_4$ composition (Ross et al., 2008; Speil & Leineweber, 1969; Zholobenko et al., 2021). Serpentine minerals, including chrysotile, are characterized by their curved shape under a microscope, whereas amphiboles exhibit a straight and rigid morphology (Castro et al., 2003). Chrysotile comprises octahedral Mg and tetrahedral Si layers that bundle together to form a fiber with the outermost layer of Mg hydroxide (Bales & Morgan, 1985; Walter et al., 2022). This natural magnesia-silicate clay mineral has a distinct fibrous or tubular nanostructure comprising silica oxide tetrahedral sheets and brucite octahedral sheets in a 1:1 stoichiometric ratio. However, the lattice sizes of these two sheets differ, resulting in curly and fibrous structures that allow for lattice matching (Dubin et al., 2013; Liu et al., 2020). Chrysotile asbestos has exceptional splitting properties, allowing it to be separated into filaments with diameters as small as 1 to 2 μm (Wang et al., 2019).

Asbestos has been used in ancient times as a fire-resistant material (Røe & Stella, 2015). Its usage has become widespread during the industrial age (Janela & Pereira, 2016), particularly in chrysotile and crocidolite forms. The valuable properties of asbestos, such as high tensile strength, heat and fire resistance, electrical insulation, and chemical inertness

(Zholobenko et al., 2021), make it ideal for use as products in construction materials, automotive components, and fireproof textiles (Bartrip, 2004; Dodson &, 2011; Hassanpour et al., 2012). Asbestos production peaked in 1977, with around 4.8 million tons produced in 25 countries (Park et al., 2012). Between 1900 and 2015, approximately 210 million tons of asbestos were extracted globally. It has been used in over 3000 different products (Harris & Kahwa, 2003; Szeszenia-Dąbrowska, 2004), including sealants, brake pads, membranes, pipes, facade panels, roof coverings, filters, clothing, and fire retardant fabrics (Iwaszko et al., 2018). Asbestos-cement products have been used in Hungary since the 1940s, predominantly as roofing sheets and pipes. The compositions of these products vary internationally. For instance, Poland classifies them as soft (containing over 20% asbestos) or hard (< 20% asbestos) (Dyczek, 2007).

In Hungary, low binder asbestos products such as blown insulation contain 95% to 97% asbestos and 3% to 5% binder. Applications with a high binder content, such as asbestos-cement flat slate, corrugated slate, and water pipes, have 8% to 10% asbestos and 90% to 92% cement binder (Tóth & Weiszburg, 2011). Table 1 summarizes the general properties and characteristics of the asbestos-cement roofing elements widely used in Hungary and prepared according to Hungarian methodologies. Asbestos-cement products in Hungary typically use various tracers and additives, typically various polysilicates and glass fiber, to improve the final physical properties of the final product. Differences between countries

Table 1

General characteristics of small and large asbestos cement roofing elements

Main properties	Small asbestos cement roofing elements	Large asbestos cement roofing elements
Asbestos content (%)	8–10	8–10
Cement content (%)	90%–92%	90%–92%
Thickness (mm)	4	5
Length (cm)	30–40	160–250
Width (cm)	30–40	93
Weight (kg/m²)	7,6	11,7
Flexural strength (MPa)	31	170
Heat resistance (°C)	200	200
Resistance to frost (°C)	-20	-20
Water absorption (%)	15	15–25
Resistance to dilute acids	No	No
Resistance to dilute brine	No	No
Resistance to oil	No	No
Resistance to petrol	No	No
Resistance to weak alkali	Yes	Yes
Thermal conductivity (W/mK)	0,65	0,651

Source: Székely et al., 1972

are clear, as Poland has asbestos fiber contents ranging from 10% to 11% for pressed flat panels, 10%–14% in corrugated sheets, and 14%–18% in asbestos-cement pipes (Dyczek, 2007; Raczko et al., 2022). Asbestos-based cement composites were installed globally in water mains, still forming a significant part of water distribution networks (Bahadori, 2016; Brandt et al., 2017; Zavašnik et al., 2022). Health concerns related to asbestos emerged in the early 20th century (Doll, 1993) and have led to its ban in many countries (Korda et al., 2017) due to associated health risks from inhaling asbestos fibers.

These risks include lung cancer, mesothelioma (Azuma et al., 2009; Currie et al., 2009; Goldberg & Luce, 2009; Zha et al., 2019), and asbestosis, with increasing related deaths (Harremoës et al., 2001; Murayama et al., 2006). The WHO (1986) defines asbestos fibers as having a length greater than 5 μm, a diameter less than 3 μm, and an aspect ratio of at least 3:1. Many health agencies have adopted this definition for asbestos fiber size (Thives et al., 2022). Asbestos materials' harmfulness and disposal challenges are now globally recognized, with over 75 countries banning their use owing to their carcinogenic potential (Santana et al., 2023; Stayner et al., 2013). Asbestos-related diseases cause around 100,000 deaths annually, including 15,000 in Europe and 12,000 in the United States (Iwaszko et al., 2018).

Despite this, asbestos-cement roofing components and artifacts remain in many buildings or are improperly disposed of in landfills (Carneiro et al., 2021). The lifespan of asbestos cement products is estimated at 30 to 40 years, though it varies due to differences in material and quality composition between countries. Punurai & Davis (2017) estimated a 70-year lifespan for asbestos-cement pipes, though, in Hungary, it is approximately 40 years, evidenced by increasing failures and pipe breaks. Scientific research on asbestos is extensive and is divided into various interdisciplinary fields, such as medicine and engineering (Thives et al., 2022). Despite the ubiquity of asbestos pollution as an environmental concern, the scientific literature remains scarce (Lisco et al., 2023). Asbestos-cement wastes pose a significant environmental challenge owing to the pathogenic properties of asbestos and the proliferation of products containing asbestos fibers (Iwaszko et al., 2018). More detailed information on fiber size and type in the environments is necessary to aid epidemiological studies. Developing and enhancing exposure metrics is crucial for accurately predicting asbestos-related disease risks (Berman & Crump, 2003). Ervik et al. (2021) analyzed asbestos fibers from a 60-year-old corrugated cement roof in Southern Norway. They discovered that numerous fibers in runoff water and weathered roof debris samples were prone to be carried away by the wind into the air and soil or washed out by rainwater (Thives et al., 2022).

Despite these findings, the number of asbestos tests conducted for environmental monitoring remains limited, with measurements primarily focused on air detection. The weathering of an asbestos cement sheet primarily depends on its main component (90%

cement), whereas the more resistant asbestos is increasingly exposed as the cement matrix wears away. As a result, weathered asbestos cement often has a higher potential to release fibers than unweathered cement, as more loosely bound fibers are exposed on the surface. In extreme cases, weathering may cause the surface to flake or crack, thereby increasing the area from which asbestos can be released into the air (Burdett, 2006). The resistance of chrysotile to acids is limited. Both the sulfuric acid in acid rain and the organic acids produced by molds, mosses, and lichens (Favero-Longo et al., 2005) interact with exposed chrysotile asbestos. Over time, these reactions progressively strip magnesium hydroxide from the chrysotile structure (Burdett, 2006; Hodgson & Darnton, 2000).

Consequently, the primary objectives of this study were (1) to determine the chrysotile content, which is a prevalent asbestos mineral (Landrigan, 1998), in several selected Hungarian-manufactured asbestos cement products, (2) to identify the trace elements present in these products, and (3) to analyze the differences in these products when exposed to or protected from environmental factors. The novelty of this research is underlined by the fact that most previous research has focused only on the qualitative characterization of asbestos (Malinconico et al., 2022; Rolfe et al., 2024; Tabata et al., 2022; Zholobenko et al., 2021). Typically, the role of trace elements, origin-specific analysis and environmental effects have been neglected segments. To achieve these goals, we employed Fourier transformation infrared (FTIR) and transmission electron microscopy (TEM) techniques on a pair of samples from each of three product groups: asbestos-cement pipes, flat slates, and corrugated slates, subjecting them to either direct environmental exposure for at least one year or hermetically sealing them to prevent exposure to the environment. We hypothesized that chrysotiles could be detected in all the asbestos cement samples, and the chrysotiles from samples exposed to environmental effects would be more easily detected because of their structural erosion. In addition, traces of specific additives were also searched, which have not been investigated by any research until now (Károly, 2022).

METHODOLOGY

Experimental Materials

Three product groups were used: (1) asbestos-cement pipes, (2) flat slates, and (3) corrugated slates. We took a pair of samples from each group, resulting in six samples. For each product group, the first sample was subjected to environmental exposure (e.g., rain and wind) for at least one year. In contrast, the second sample was hermetically sealed and protected from external influences. This approach allowed us to compare the effects of environmental exposure on each product group with their respective sealed counterparts.

The first pair of samples, an asbestos cement corrugated plate (ACCP-1 and ACCP-2), was approximately 30 years old and originated in a cement factory in Hungary. The plates exhibited typical erosion and damage.

Gergely Zoltán Macher, Fanni Károly, Christopher Teh Boon Sung, Dóra Beke, András Torma and Szilveszter Gergely

The second pair of samples were asbestos cement slates (ACF-1 and ACF-2), both approximately 20 to 25 years old, eroded and damaged by surface corrosion.

The third pair of samples, ACP-1 and ACP-2, were unassembled and unused products aged 30 to 40. They also originated from a cement factory in Hungary. Both the ACP-1 and ACP-2 pipes were physically well-structured, without extensive cracks and corroded, eroded surfaces.

Before each analysis, all three pairs of samples were thoroughly cleaned with distilled water and isopropyl to remove contaminants that could bias the results. The samples were then cut to similar sizes and densities, and each piece was cast with multi-component epoxy resin and polished into disks of the same size. All samples are shown in Figure 1. The main characteristics of the tested samples are summarized in Table 2.

All asbestos shows intense absorption in the 1200–900 cm^{-1} range and 600–300 cm^{-1}. Recording the spectrum up to 200 cm^{-1} provides all the necessary information for qualitative
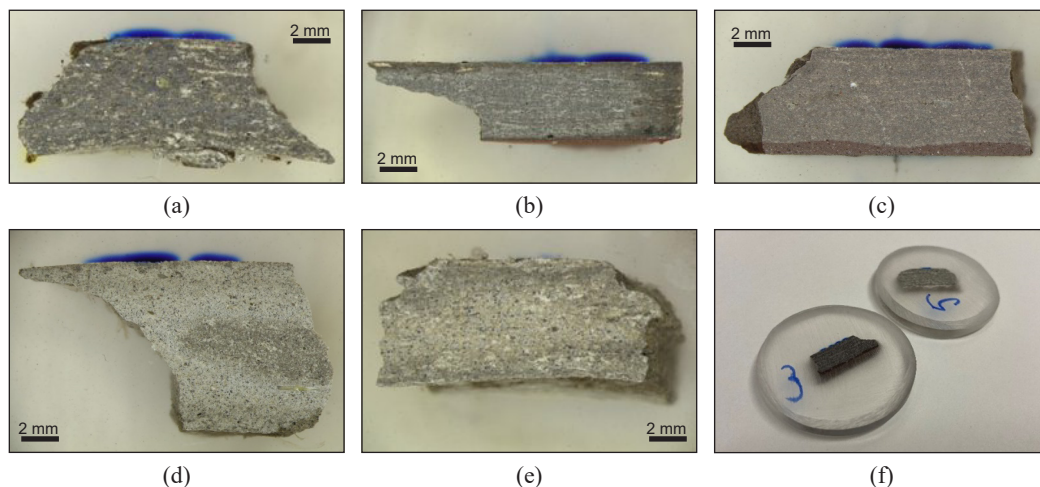

Figure 1. Asbestos cement waste samples. From left to right, beginning from the top: (a) ACCP-1 asbestos cement corrugated plate; (b) ACF-1 asbestos cement slate (isolated); (c) ACF-2 asbestos cement slate (exposed); (d) ACP-1 asbestos cement pipe (isolated); (e) ACP-2 asbestos cement pipe (exposed); (f) prepared samples.

Table 2
Characteristics of the analyzed samples

ID	Product type	Product age	Exposed or Isolated
ACCP-1	Asbestos cement corrugated plate	30 years old	Isolated
ACCP-2	Asbestos cement corrugated plate	30 years old	Exposed
ACF-1	Asbestos cement slate	20 to 25 years old	Isolated
ACF-2	Asbestos cement slate	20 to 25 years old	Exposed
ACP-1	Asbestos cement pipe	30 to 40 years old	Isolated
ACP-2	Asbestos cement pipe	30 to 40 years old	Exposed

identification of the asbestos type. Chrysotile differs significantly from amphiboles in that it shows intense double hydroxyl groups at 3693 cm^{-1} and 3648 cm^{-1}, formed between layers of hydroxyl groups located between the main silicate layers of the lattice. Chrysotile can be quantified from its absorption at 3690 cm^{-1} in the absence of anthophyllite (Károly, 2022).

Sample Preparation and the Used Instrument

Macro measurements were performed using a PerkinElmer Spotlight 400 (PerkinElmer, MA, US) device. For such an examination, the samples were carefully prepared, and broken pieces of asbestos-cement products were poured into an epoxy resin solution for preparation and then polished to make their cross-section easier to examine. The samples were cleaned with distilled water treatment; the treatment itself would have distorted the investigation of the role of environmental effects. Pouring with epoxy resin uses a mold according to the specified dimensions. The discs were ground with a grinder to achieve a disc range of 30 × 5 mm. The resulting 30 × 5 mm discs were placed on the slide of the instrument, where the material could be examined with a 0.3-mm germanium crystal facing downwards so that the selected area of the sample could be scanned with infrared rays, resulting in the creation of an absorption map of the material. From this map, different spectra are marked with different colors, which point to specific materials in the spectrum library, thus making the components identifiable.

The PerkinElmer Spectrum 400 (PerkinElmer, MA, U.S.) machine was used to perform the microscopic measurements. For these measurements, we took samples from broken sections of asbestos cement products and collected scrap samples from the matrix material to analyze their composition, particularly for additives. Subsequently, these materials were then positioned on the object table of the spectroscope, specifically on a 0.3-mm diamond crystal facing upwards. A force of approximately 100 N was then applied to secure the materials for the analysis. These tests were sensitive to moisture and carbon dioxide; therefore, before each measurement, the spectrum of the environmental background had to be recorded first so that the instrument could distinguish between the true and background spectrum of the sample.

RESULTS AND DISCUSSION

Therefore, in our research, we conducted targeted analyses to verify the chrysotile content of asbestos-cement products and the role of environmental exposure in influencing emissions. In addition to chrysotile content, we looked for trace elements such as glass fiber and polysilicate content, which were typically the main excipients of products manufactured in Hungary.

Therefore, we are looking for answers to two main questions: (1) Can the role of environmental impact be demonstrated by infrared technology? And (2) Is it possible to perform an origin-specific analysis of these products using infrared technology?

Detection of Chrysotile Asbestos

All asbestos exhibits intense absorption in the 1200-900 cm^{-1} and 600–300 cm^{-1} range. Weaker characteristic bands were also observed between 850–600 cm^{-1}. All information for qualitative identification of the asbestos type can be obtained by recording the spectrum up to 200 cm^{-1}. A slight absorption was observed around 3700–3200 cm^{-1} and 1700–1400 cm^{-1}. Chrysotile differs markedly from amphiboles because it shows intense double hydroxyl groups at 3693–3648 cm^{-1}, formed between layers of hydroxyl groups between the main silicate layers of the lattice. This band characterized and quantified fibers in liquid samples saturated with dust or asbestos fibers.

The band is sensitive to interference from other silicate minerals, such as talc, kaolinite, and montmorillonite, which are widely used in industry. The forms of chrysotile, amosite, anthophyllite and crocidolite can be identified separately by infrared spectroscopy. Chrysotile was quantified by its absorbance at 3690 cm^{-1} in the absence of anthophyllite. Anthophyllite was detected at 670 cm^{-1} in the absence of talc. The amosite, crocidolite, and anthophyllite absorption bands at 775 cm^{-1} could be used for quantitative analysis.

Detection of Chrysotile from Asbestos Cement Corrugated Plates

The corrugated asbestos cement plate is a high-binder asbestos-cement product; thus, its asbestos content was close to 8%–10%, with a corresponding cement content above 90%. The corrugated sheet (ACCP-1) under investigation had been exposed to environmental influences originating from construction and demolition activities, but the structure did not appear to have been extensively damaged by weathering. Its surface was rough, similar to cement, and its color was greyish brown. The sample structure was robust and hard, with asbestos fibers clearly visible, arranged in thin bundles, such as individual fibers, intermingled with the cement mixture. The fibers could only be pulled out along the fracture. Table 3 contains the results obtained from the instrument's spectral library supplemented with asbestos spectra.

Table 3
Concordance rates for chrysotile from asbestos cement corrugated plates

Range	Search Reference	Search Reference Spectrum Description	Match
Full range	**RESTAURO- ID0344**	**IMP00280.SP IMP00280 CHRYSOTILE, SI-NMNH, #107853, PMA, TRAN**	**68.4%**
	PERKIN~1- PO0265	GOMMA NBR + PVC + PLASTIFICANTE	66.1%
	PERKIN~4- GS0005	ACRILONITRILE	64.8%
1800-650 cm^{-1}	**RESTAURO- ID0344**	**IMP00280.SP IMP00280 CHRYSOTILE, SI-NMNH, #107853, PMA, TRAN**	**71.5%**
	PERKIN~1- PO0265	GOMMA NBR + PVC + PLASTIFICANTE	70.9%
	PERKIN~1- PO0264	GOMMA NBR + PVC + PLASTIFICANTE + TALCO	67.7%

Determining chrysotile asbestos in practice can be very challenging; therefore, even a hit rate above 50%–60% is decisive enough to be accepted as identification. The chrysotile was identified with 68.41% certainty over the whole range (Table 1). There was a lower probability of plastic derivatives and nitrile compounds being found, which could have been absorbed from the matrix material into the fibers. In the 1800–650 cm^{-1} band, the third hit was asbestos derivatives with 65.79% certainty, but the results also included plasticizers and talc. Based on these values, it can be stated that chrysotile was clearly detectable in the corrugated plate.

Detection of Chrysotile from Asbestos Cement Flats

The test samples for flat shale analysis included (1) from an environmentally exposed shale (ACF-1) and (2) from a preserved shale (ACF-2). It was assumed that asbestos fibers would be more securely incorporated into the matrix material of the preserved product, making them more difficult to detect. In contrast, owing to structural degradation, we anticipated more easily detectable results from the eroded asbestos slate.

The first flat shale sample was an environmentally exposed asbestos product, with its characteristic layered shape clearly visible owing to the manufacturing processes. A staggered detachment pattern emerged when broken, which could be attributed to weathering delamination, causing the plates to separate slightly. The surface was smooth, firm to touch, and harder than the other samples, and the shale contained coarser fragments scattered throughout its non-homogeneous structure. Asbestos fibers in the sample were clearly visible as thinner bundles, with individual fibers being less discernible or not visible at all. Here, asbestos was removed using tweezers, and the fibers were not easily separated from the binder. The search results of the obtained spectra are listed in Table 4.

These results were similar to those of the corrugated plate measurement (Table 1) but with a higher degree of agreement, as chrysotile had a 70% greater probability of being the first hit in both instances. The second asbestos mound tested, which was not affected

Table 4

Concordance rates for chrysotile from asbestos cement flats

Range	Search Reference	Search Reference Spectrum Description	Match
Full range	**RESTAURO- ID0344**	**IMP00280.SP IMP00280 CHRYSOTILE, SI-NMNH, #107853, PMA, TRAN**	**74.0%**
	PERKIN~4- GS0005	ACRILONITRILE	69.5%
	PERKIN~1- PO0264	GOMMA NBR + PVC + PLASTIFICANTE + TALCO	61.3%
1800-650 cm^{-1}	**RESTAURO- ID0344**	**IMP00280.SP IMP00280 CHRYSOTILE, SI-NMNH, #107853, PMA, TRAN**	**73.2%**
	PERKIN~1- PO0264	GOMMA NBR + PVC + PLASTIFICANTE + TALCO	65.6%
	PERKIN~1- PO0265	GOMMA NBR + PVC + PLASTIFICANTE	65.1%

by environmental influences over the years, was denser, had a higher amount of matrix material, and featured a harder texture compared to the other material.

The asbestos fibers in the sample appear arranged individually rather than as bundles, giving it an almost hair-like appearance. Despite the large number of fibers, their distribution was homogeneous. These fibers were firmly embedded in the mixture, making them difficult to extract as they either broke or slipped out of the tweezers during preparation. Due to these factors, chrysotile was not detected in Sample 3.

Detection of Chrysotile from Asbestos Cement Pipes

Similar to the artificial shale, two samples of asbestos-cement pipes were tested to analyze the effect of environmental exposure on the structure. The first test pipe, a large cross-section asbestos cement pipe (ACP-1), was exposed to environmental effects. Its structure was not homogeneous, but it had smaller and darker to lighter grains appearing in the light-base color of the matrix material. The asbestos fibers were well-defined, arranged in islands, dense bundles, and were clearly visible in their bright white color. They were the easiest samples to cut out and handle and tended to splinter rather than tear. The spectral library hits for these samples are listed in Tables 5 and 6.

Based on the results, the most reliable evidence for the presence of chrysotile was 86.7% and 89.88%, respectively. The plastic derivative, previously detected, was also present, as was polysilicate, a type of sodium silicate found in cements and refractories. This substance could be explained by the fact that, during production, the compound was absorbed into the porous fibers of the asbestos or the fiber bundles. With a smaller cross-section, the second pipe was an asbestos product protected from environmental influences. Its fracture was staggered, similar to that of shale stored under similar conditions, with layers of delamination observed. The texture was similar to textiles; it was rough, highly textured, and much lighter in color than the other test materials.

This tube was the most heterogeneous of the samples, with various darker to lighter patches mixed with the binder. The asbestos bundles were clearly visible, but the number

Table 5

Concordance rates for chrysotile from asbestos cement pipe (ACP-1)

Range	Search Reference	Search Reference Spectrum Description	Match
Full range	**RESTAURO- ID0344**	**IMP00280.SP IMP00280 CHRYSOTILE, SI-NMNH, #107853, PMA, TRAN**	**86.7%**
	PERKIN~1- PO0265	GOMMA NBR + PVC + PLASTIFICANTE	74.4%
	POLYMER - HU1137	POLYSILICATE 1.7/250MG KBR 0-00-0	71.1%
1800-650 cm^{-1}	**RESTAURO- ID0344**	**IMP00280.SP IMP00280 CHRYSOTILE, SI-NMNH, #107853, PMA, TRAN**	**89.9%**
	PERKIN~1- PO0265	GOMMA NBR + PVC + PLASTIFICANTE	80.9%
	TRANSM~1- HU1137	POLYSILICATE 1.7/250MG KBR 0-00-0	77.5%

Table 6

Concordance rates for chrysotile from asbestos cement pipe (ACP-2)

Range	Search Reference	Search Reference Spectrum Description	Match
Full range	**RESTAURO- ID0344**	**IMP00280.SP IMP00280 CHRYSOTILE, SI-NMNH, #107853, PMA, TRAN**	**59.6%**
	PERKIN~4- GS0005	ACRILONITRILE	66.3%
	PERKIN~3- IN0016	FIBRA DI VETRO STRAND G	63.5%
	RESTAURO- ID0365	IMP00301.SP IMP00301 CHROME YELLOW, PBS04 + PB CR04, FORBES, SCC, TRAN	63.3%
	PERKIN~3- IN0028	VETRO - ATR DI GERMANIO	63.1%
	PERKIN~1- PO0265	GOMMA NBR + PVC + PLASTIFICANTE	60.5%
1800-650 cm^{-1}	TRANSM~1- GS0017	C2H4-4 100% ETHEN; D=10CM; NACL	69.8%
	PERKIN~3- IN0028	VETRO - ATR DI GERMANIO	69.4%
	RESTAURO- ID0221	IMP00157.SP IMP00157 CHROME GREEN, FORBES: ROWNEY, PMA# I-40, PMA, TRAN	67.6%
	TRANSM~1- GS0018	C2H4-5 100 % ETHEN; D=2CM; BAF2	66.1%
	PERKIN~3- IN0016	FIBRA DI VETRO STRAND G	66.0%

of asbestos bundles appeared to be smaller than in the previously tested samples. The fine particles were scattered. The fibers were easily held with tweezers; however, extraction was not as easy as before, and they were torn along the fracture line, as in the large pipe, with the mineral fibers fluffed up. Although asbestos fibers were not difficult to extract from the fifth sample, chrysotile came in a mere sixth of the hit list, with only 59.61%. No results were obtained from the characteristic peak band, but both yielded a higher probability of glass fiber.

Acrylonitrile, fiberglass, and plastic derivatives, which had previously been found, appeared in the full range, with yellow pigment material as an additional element on the list. In addition, several hits that did not appear in the previously analyzed hits, such as ethene, whose origin was unknown. It may have been deposited over the years.

Detection of Glass Fibers

In manufacturing these products, a mixture of 20% to 30% by weight of expanded perlite with a grain size of 0.5 mm and 20% to 80% by weight of silica fume is suspended. Spongy silica is sometimes used instead of hard earth, where at least 98% by weight of material with a grain size of up to 0.2 mm is used. The mixture also contains preferably 1.3% to 1.5% by weight of cellulose (Lejsek et al., 1976).

Glass fiber was detected in several samples of asbestos fibers and scrapings. It was found in the corrugated slate, the first environmentally exposed flat slate, and the small cross-section asbestos cement tube (Table 7). The upper half of Table 7 displays the spectral analysis of the asbestos fibers, whereas the lower half shows the glass fiber detected in the matrix material sample. In all cases, the agreement was above 55.0%.

Gergely Zoltán Macher, Fanni Károly, Christopher Teh Boon Sung, Dóra Beke, András Torma and Szilveszter Gergely

There are several possible explanations for its presence. The use of asbestos-cement products led to increasing demands in terms of fire resistance and structural performance. In 1976, a new patent was granted to address these needs. The proposed technology involved sifting well-known asbestos cement containing up to 55 wt% (weight percent) asbestos through a sieve with a mesh size of 1.35 mm to obtain a residue of at least 40 wt%. Then, a quartz content of 3–50 wt%, consisting of expanded perlite and silica fume, was added. Lastly, 3 wt% of inorganic fibrous material, an asbestos-glass fiber suspension, was included, with the glass fiber length preferably being 10 mm. Additionally, 1.3–1.5 wt% cellulose might be required (Lejsek et al., 1976).

The advantage of altering the composition was achieving the desired strength while maintaining a low bulk density and high porosity. It was accomplished by reducing the amount of cement binder and increasing the filler. Table 8 compares the bending tests of two previously manufactured, unnamed asbestos-cement formulations and the new formulation (Lejsek et al., 1976). The test was used to determine the maximum stress and load capacity. Based on the data, it can be concluded that the glass fiber-reinforced product had a much lower bulk density compared to its predecessors. However, its relative bending strength parallel and perpendicular to the fibers was more favorable, making the material more robust. In accordance with the standards for asbestos cement, eight random samples

Table 7

Concordance rates for glass fibers from asbestos cement wastes

Range	Sample	Search Reference	Search Reference Spectrum Description	Match
Full range	ACP-2- asbestos	PERKIN~3- IN0016	FIBRA DI VETRO STRAND G	63.5%
	ACF-1 - asbestos	PERKIN~3- IN0016	FIBRA DI VETRO STRAND G	59.9%
1800-650 cm^{-1}	ACP-2 - asbestos	PERKIN~3- IN0016	FIBRA DI VETRO STRAND G	66.0%
	ACF-1 - asbestos	PERKIN~3- IN0016	FIBRA DI VETRO STRAND G	61.7%
	ACCP-1 - asbestos	PERKIN~3- IN0016	FIBRA DI VETRO STRAND G	57.1%
Full range	ACF-1 - cement	PERKIN~3- IN0016	FIBRA DI VETRO STRAND G	63.2%
1800-650 cm^{-1}	ACF-1 – cement	PERKIN~3- IN0016	FIBRA DI VETRO STRAND G	63.5%

Table 8

Flexural strength testing of asbestos cement products enriched with glass fibers (Lejsek et al., 1976)

Property	Asbestos cement containing glass fiber	Previously used asbestos cement	
Volumetric weight (kPa m^{-3})	650	796	741
Flexural strength parallel to the elementary fibers (kp cm^{-2})	105	92.2	113.7
Flexural strength perpendicular to the elementary fibers (kp cm^{-2})	65–70	72.9	104.9

were taken from every 50,000 pieces produced and tested. For the flexural strength test, 22 cm long, 10 cm wide rectangular elements were prepared, and both perpendicular and parallel samples were tested. The analysis was preceded by 28 days of air-dry confinement (Fügedi, 1986).

Detection of Polysilicate (Water Glass)

Sodium silicate, commonly known as water glass, exists in ortho-, meta-, poly-, and pyrosilicate forms. When mixed with cement, sodium silicate enhances thermal resistance, and when added to adhesives, it improves the thermal resistance of the bonding surface. Another benefit of its use is that it can prevent water infiltration into the material by blocking moisture from entering the pores when used as a surface treatment agent. It also has flame-retardant and fire-resistant properties, as it releases water when heated, which cools the surface. All these characteristics have made it a popular additive in the fire protection, woodworking, and construction industries (Grote, 1897).

The first mention of the role of polysilicates in asbestos production dates to 1896 in a patent by Lajos Grote. In his patent, he described a manufacturing process for asbestos products where the fibers were impregnated with a mixture of water glass, glue and formaldehyde solution. The process involved dissolving one part of glue in 12 parts of boiling water, mixing the cooled solution with six parts of water glass solution, and finally adding 7–9 parts of 40% formaldehyde. The asbestos fibers were soaked in this mixture until they saturated sufficiently. The resulting asbestos products dried and hardened in about 12 hours, after which they were ready for machining (Grote, 1897).

The results obtained for the asbestos cement corrugated plates, flat slates, and pipes consistently showed the presence of polysilicate, or water glass, in both ranges. In all measurements, the extracted asbestos fibers indicated the presence of the compound, which could be due to the absorption of material into porous fibers. The spectral agreement was above 60.0% in all cases except one. The pipe measured the highest values, while the lowest was obtained in the slate. The detailed results can be seen in Table 9.

Table 9
Concordance rates for polysilicate from asbestos cement wastes

Range	Sample	Search Reference Spectrum Description		Match
Overlap	ACCP-1	POLYSILICATE 1.7/250MG KBR	0-00-0	60.2%
	ACF-1	POLYSILICATE 1.7/250MG KBR	0-00-0	57.8%
	ACP-1 -asbestos	POLYSILICATE 1.7/250MG KBR	0-00-0	66.6%
	ACP-2 -asbestos	POLYSILICATE 1.7/250MG KBR	0-00-0	67.2%
1800-650 cm^{-1}	ACCP-1 - asbestos	POLYSILICATE 1.7/250MG KBR	0-00-0	60.5%
	ACP-1 - asbestos	POLYSILICATE 1.7/250MG KBR	0-00-0	74.4%
	ACP-2 - asbestos	POLYSILICATE 1.7/250MG KBR	0-00-0	75.6%

CONCLUSION

Chrysotile asbestos (white asbestos) was detected in all the tested product-waste groups with a relatively high hit rate and agreement—the presence of chrysotile in each sample tested, with spectral matches ranging from 59.6% to 86.7%. A particularly significant finding was that removing asbestos from asbestos-cement products exposed to environmental influences was easier, and the degree of agreement between the results was higher than that for products sealed off from such effects. The presence of chrysotile was much easier to detect for the environmentally exposed AC pipe compared with the sealed samples. However, contrary to expectations, a higher degree of agreement with chrysotile was demonstrated when examining the AC pipes than when measuring the flat or corrugated shale slate samples. The match rate with the chrysotile spectrum ranged from 86.7 to 89.9% for the AC pipe exposed to the environment. This compares to 59.6% for all samples that were isolated and spared from environmental influence.

Additionally, we established that all asbestos cement products contained glass fibers, with an average spectral match of 62.1%. Our analysis showed an average spectral match of 66.0% in the case of polysilicates, which were classified as very typical additives in Hungary during the production period of the products. Overall, using infrared technology principles, chrysotile (white asbestos) was detected in all examined products and waste groups. A key implication of this research is that environmental influences make white asbestos fibers easier to detect and separate than sealed-off products. Another important implication is that FT-IR technology can also be used to determine the inherent specific character of these products. However, the lack of a uniform patent and methodology, as well as the difficulty of testing asbestos-cement products, are major limitation factors to research. Our analyses were based on samples currently common in Hungary, but the work can be adapted to other countries. We aim to broaden the spectrum of this research in the future, carry out comparative studies by testing products manufactured abroad, and develop a methodology.

ACKNOWLEDGEMENT

REFERENCES

Azuma, K., Uchiyama, I., Chiba, Y., & Okumura, J. (2009). Mesothelioma risk and environmental exposure to asbestos: Past and future trends in Japan. *International Journal of Occupational and Environmental Health*, *15*(2), 166–172. https://doi.org/10.1179/oeh.2009.15.2.166

Bahadori, A. (2016). Chapter 8 - Water supply and distribution systems. In A. Bahadori (Ed.), *Essentials of Oil and Gas Utilities* (pp. 225–328). Elsevier. https://doi.org/10.1016/B978-0-12-803088-2.00008-0

Bales, R. C., & Morgan, J. J. (1985). Dissolution kinetics of chrysotile at pH 7 to 10. *Geochimica et Cosmochimica Acta*, *49*(11), 2281–2288. https://doi.org/10.1016/0016-7037(85)90228-5

Bartrip, P. W. J. (2004). History of asbestos related disease. *Postgraduate Medical Journal*, *80*(940), 72–76. https://doi.org/10.1136/pmj.2003.012526

Berman, D., & Crump, K. (2003). *Technical Support Document for a Protocol to Assess Asbestos-related Risk*. U.S. Environmental Protection Agency.

Brandt, M. J., Johnson, K. M., Elphinston, A. J., & Ratnayaka, D. D. (2017). Chapter 7 - Chemistry, microbiology and biology of water. In M. J. Brandt, K. M. Johnson, A. J. Elphinston & D. D. Ratnayaka (Eds.), *Twort's Water Supply* (pp. 235–321). Elsevier. https://doi.org/10.1016/B978-0-08-100025-0.00007-7

Burdett, G. (2006). *Investigation of the Chrysotile Fibres in an Asbestos Cement Sample*. Health & Safety Laboratory.

Carneiro, G. O., Santos, T. A., Simonelli, G., Ribeiro, D. V., Cilla, M. S., & Dias, C. M. R. (2021). Thermal treatment optimization of asbestos cement waste (ACW) potentializing its use as alternative binder. *Journal of Cleaner Production*, *320*, Article 128801. https://doi.org/10.1016/j.jclepro.2021.128801

Castro, H., Giannasi, F., & Novello, C. (2003). A luta pelo banimento do amianto nas Américas: Uma questão de saúde pública [The struggle to ban asbestos in the Americas: A public health issue]. *Ciência & Saúde Coletiva*, *8*(4), 903–911. https://doi.org/10.1590/S1413-81232003000400013

Currie, G. P., Watt, S. J., & Maskell, N. A. (2009). An overview of how asbestos exposure affects the lung. *BMJ*, *339*, Article b3209. https://doi.org/10.1136/bmj.b3209

Dodson, R. F., & Hammar, S. P. (2011). *Asbestos - Risk assessment, epidemiology, and health effects* (2nd ed.). CRC Press. https://doi.org/10.1201/b10958

Doll, R. (1993). Mortality from lung cancer in asbestos workers 1955. *Occupational and Environmental Medicine*, *50*(6), 485–490. https://doi.org/10.1136/oem.50.6.485

Dubin, H., Xi, C., & Xiu-yun, C. (2013). Structure performance and application research of natural nano-tubular chrysotile. *Journal of Functional Biomaterials*, *44*(14), 1984-1989. https://doi.org/10.3969/j.issn.1001-9731.2013.14.002

Dyczek, J. (2007). *Bezpieczne postępowanie z azbestem i materiałami zawierającymi azbest : Szkoła "Azbest - bezpieczne postępowanie"* [*Safe Handling of Asbestos and Materials Containing Asbestos: School of "Asbestos - safe handling"*]. Wydawnictwo Naukowe.

Ervik, T., Hammer, S. E., & Graff, P. (2021). Mobilization of asbestos fibers by weathering of a corrugated asbestos cement roof. *Journal of Occupational and Environmental Hygiene*, *18*(3), 110–117. https://doi.org/10.1080/15459624.2020.1867730

Favero-Longo, S. E., Turci, F., Tomatis, M., Castelli, D., Bonfante, P., Hochella, M. F., Piervittori, R., & Fubini, B. (2005). Chrysotile asbestos is progressively converted into a non-fibrous amorphous material by the chelating action of lichen metabolites. *Journal of Environmental Monitoring*, *7*(8), 764-766. https://doi.org/10.1039/b507569f

Goldberg, M., & Luce, D. (2009). The health impact of nonoccupational exposure to asbestos: What do we know? *European Journal of Cancer Prevention*, *18*(6), 489–503. https://doi.org/10.1097/CEJ.0b013e32832f9bee

Grote, L. (1897). *Eljárás plasztikus testeknek azbesztrostokból vagy azbesztgyártmányokból való előállítására* [*Process for the production of plastic bodies from asbestos fibers or asbestos products*] (Patent 8094). Magyar Királyi Szabadalmi Hivatal.

Harremoës, P., Gee, D., MacGarvin, M., Stirling, A., Keys, J., Wynne, B., & Guedes, V. S. (2001). *Late lessons from early warnings: The precautionary principle 1896-2000* (Report No. 22 Enviroment Issue). European Environment Agency.

Harris, L., & Kahwa, I. (2003). Asbestos: Old foe in 21st century developing countries. *The Science of The Total Environment*, *307*(1–3), 1–9. https://doi.org/10.1016/S0048-9697(02)00504-1

Hassanpour, M., Shafigh, P., & Mahmud, H. Bin. (2012). Lightweight aggregate concrete fiber reinforcement – A review. *Construction and Building Materials*, *37*, 452–461. https://doi.org/10.1016/j.conbuildmat.2012.07.071

Hodgson, J. T., & Darnton, A. (2000). The quantitative risks of mesothelioma and lung cancer in relation to asbestos exposure. *The Annals of Occupational Hygiene*, *44*(8), 565–601. https://doi.org/10.1093/annhyg/44.8.565

Iwaszko, J., Zawada, A., Przerada, I., & Lubas, M. (2018). Structural and microstructural aspects of asbestos-cement waste vitrification. *Spectrochimica Acta Part A: Molecular and Biomolecular Spectroscopy*, *195*, 95–102. https://doi.org/10.1016/j.saa.2018.01.053

Janela, J. M. E. M., & Pereira, P. J. S. (2016). História do amianto no mundo e em Portugal [History of asbestos in the world and in Portugal]. *CEM Cultura, Espaço & Memória, 7*, 93-206.

Korda, R. J., Clements, M. S., Armstrong, B. K., Law, H. Di, Guiver, T., Anderson, P. R., Trevenar, S. M., & Kirk, M. D. (2017). Risk of cancer associated with residential exposure to asbestos insulation: A whole-population cohort study. *The Lancet Public Health*, *2*(11), e522–e528. https://doi.org/10.1016/S2468-2667(17)30192-5

Kusiorowski, R., Lipowska, B., Kujawa, M., & Gerle, A. (2023). Problem of asbestos-containing wastes in Poland. *Cleaner Waste Systems*, *4*, Article 100085. https://doi.org/10.1016/j.clwas.2023.100085

Landrigan, P. J. (1998). Asbestos — Still a carcinogen. *The New England Journal of Medicine*, *338*(22), 1618–1619. https://doi.org/10.1056/NEJM199805283382209

Lavento, M., & Hornytzkyj, S. (1995). On asbestos used as temper in Finnish subneolithic, neolithic and early metal period pottery. *Fennoscandia Archaeologica, 12*, 71-75.

Lejsek, L., Vichta, A., Zboril, F., Kovar, J., Fridal, J., Franc, V., & Knezek, J. (1976). *Eljárás tűzálló, állandó térfogatú azbesztcementelemek előállítására* [*Process for the production of refractory, constant volume asbestos cement elements*] (Patent 170236). Magyar Népköztársaság Országos Találmányi Hivatal.

Lisco, S., Lapietra, I., Laviano, R., Mastronuzzi, G., Fracchiolla, T., & Moretti, M. (2023). Sedimentological features of asbestos cement fragments in coastal environments (Taranto, southern Italy). *Marine Pollution Bulletin*, *187*, Article 114469. https://doi.org/10.1016/j.marpolbul.2022.114469

Liu, Q., Peng, H., Tian, X., & Guo, J. (2020). Synthesis of chrysotile based nanocomposites for tuning band gap and photocatalytic property. *Applied Clay Science*, *199*, Article 105885. https://doi.org/10.1016/j.clay.2020.105885

Malinconico, S., Paglietti, F., Serranti, S., Bonifazi, G., & Lonigro, I. (2022). Asbestos in soil and water: A review of analytical techniques and methods. *Journal of Hazardous Materials*, *436*, Article 129083. https://doi.org/10.1016/j.jhazmat.2022.129083

Misseri, M. (2023). Nucleation of naturally occurring calcic amphibole asbestos. *Environmental Research*, *230*, Article 114940. https://doi.org/10.1016/j.envres.2022.114940

Murayama, T., Takahashi, K., Natori, Y., & Kurumatani, N. (2006). Estimation of future mortality from pleural malignant mesothelioma in Japan based on an age-cohort model. *American Journal of Industrial Medicine*, *49*(1), 1–7. https://doi.org/10.1002/ajim.20246

Park, E. K., Takahashi, K., Jiang, Y., Movahed, M., & Kameda, T. (2012). Elimination of asbestos use and asbestos-related diseases: An unfinished story. *Cancer Science*, *103*(10), 1751–1755. https://doi.org/10.1111/j.1349-7006.2012.02366.x

Punurai, W., & Davis, P. (2017). Prediction of asbestos cement water pipe aging and pipe prioritization using monte Carlo simulation. *Engineering Journal*, *21*(2), 1–13. https://doi.org/10.4186/ej.2017.21.2.1

Raczko, E., Krówczyńska, M., & Wilk, E. (2022). Asbestos roofing recognition by use of convolutional neural networks and high-resolution aerial imagery. Testing different scenarios. *Building and Environment*, *217*, Article 109092. https://doi.org/10.1016/j.buildenv.2022.109092

Ristić, M., Czakó-Nagy, I., Musić, S., & Vértes, A. (2011). Spectroscopic characterization of chrysotile asbestos from different regions. *Journal of Molecular Structure*, *993*(1–3), 120–126. https://doi.org/10.1016/j.molstruc.2010.10.005

Røe, O. D., & Stella, G. M. (2015). Malignant pleural mesothelioma: History, controversy and future of a manmade epidemic. *European Respiratory Review*, *24*(135), 115–131. https://doi.org/10.1183/09059180.00007014

Rolfe, M., Hayes, S., Smith, M., Owen, M., Spruth, M., McCarthy, C., Forkan, A., Banerjee, A., & Hocking, R. K. (2024). An AI based smart-phone system for asbestos identification. *Journal of Hazardous Materials*, *463*, Article 132853. https://doi.org/10.1016/j.jhazmat.2023.132853

Ross, M., Langer, A. M., Nord, G. L., Nolan, R. P., Lee, R. J., Van Orden, D., & Addison, J. (2008). The mineral nature of asbestos. *Regulatory Toxicology and Pharmacology*, *52*(1), S26–S30. https://doi.org/10.1016/j.yrtph.2007.09.008

Santana, H. A., Júnior, N. S. A., Carneiro, G. O., Ribeiro, D. V., Cilla, M. S., & Dias, C. M. R. (2023). Asbestos-cement wastes as supplementary precursors of NaOH-activated binders. *Construction and Building Materials*, *364*, Article 129921. https://doi.org/10.1016/j.conbuildmat.2022.129921

Speil, S., & Leineweber, J. P. (1969). Asbestos minerals in modern technology. *Environmental Research*, *2*(3), 166–208. https://doi.org/10.1016/0013-9351(69)90036-X

Stayner, L., Welch, L. S., & Lemen, R. (2013). The worldwide pandemic of asbestos-related diseases. *Annual Review of Public Health*, *34*(1), 205–216. https://doi.org/10.1146/annurev-publhealth-031811-124704

Szeszenia-Dąbrowska, N. (2004). *Azbest - ekspozycja zawodowa i środowiskowa - skutki, profilaktyka* [Asbestos - Occupational and environmental exposure - Effects, prevention]. Oficyna Wydawnicza Instytut Medycyny.

Székely, L., Scharle, Gy., Betlehem, A. (1972). *Segédlet a szakipari munkák tervezéséhez és kivitelezéséhez* [Guide to planning and carrying out specialist works]. Építésügyi Tájékoztatási Központ.

Tabata, M., Fukuyama, M., Yada, M., & Toshimitsu, F. (2022). On-site detection of asbestos at the surface of building materials wasted at disaster sites by staining. *Waste Management, 138,* 180–188. https://doi.org/10.1016/j.wasman.2021.11.039

Thives, L. P., Ghisi, E., Thives Júnior, J. J., & Vieira, A. S. (2022). Is asbestos still a problem in the world? A current review. *Journal of Environmental Management*, *319*, Article 115716. https://doi.org/10.1016/j.jenvman.2022.115716

Tóth, E., & Weiszburg, T. (2011). *Környezeti ásványtan* [*Environmental Mineralogy*]. Typotex Kiadó.

Virta, R. L. (2005). *Mineral commodity profiles-asbestos: U.S. geological survey circular 1255-KK*. USGS Science for a Changing World. http://www.usgs.gov/pubprod

Walter, M., Geroldinger, G., Gille, L., Kraemer, S. M., & Schenkeveld, W. D. C. (2022). Soil-pH and cement influence the weathering kinetics of chrysotile asbestos in soils and its hydroxyl radical yield. *Journal of Hazardous Materials*, *431*, Article 128068. https://doi.org/10.1016/j.jhazmat.2021.128068

Wang, Y., Huo, T., Feng, C., Zeng, Y., Yang, J., Zhang, X., Dong, F., & Deng, J. (2019). Chrysotile asbestos induces apoptosis via activation of the p53-regulated mitochondrial pathway mediated by ROS in A549 cells. *Applied Clay Science*, *182*, Article 105245. https://doi.org/10.1016/j.clay.2019.105245

WHO (1986). *Asbestos and other natural mineral fibres*. World Health Organization. https://apps.who.int/iris/handle/10665/37190

Zavašnik, J., Šestan, A., & Škapin, S. (2022). Degradation of asbestos – Reinforced water supply cement pipes after a long-term operation. *Chemosphere*, *287*, Article 131977. https://doi.org/10.1016/j.chemosphere.2021.131977

Zha, L., Kitamura, Y., Kitamura, T., Liu, R., Shima, M., Kurumatani, N., Nakaya, T., Goji, J., & Sobue, T. (2019). Population-based cohort study on health effects of asbestos exposure in Japan. *Cancer Science*, *110*(3), 1076-1084. https://doi.org/10.1111/cas.13930

Zholobenko, V., Rutten, F., Zholobenko, A., & Holmes, A. (2021). In situ spectroscopic identification of the six types of asbestos. *Journal of Hazardous Materials*, *403*, Article 123951. https://doi.org/10.1016/j.jhazmat.2020.123951